Microstructure and Properties of Nippon Fire-Resistant Steels

W. Sha, F.S. Kelly, and Z.X. Guo

(Submitted 1 March 1999; in revised form 19 May 1999)

The microstructure and mechanical properties of two fire-resistant steels manufactured by Nippon Steel were investigated. Microstructural observation was carried out using optical microscopy, transmission electron microscopy (TEM), and scanning electron microscopy (SEM). It was found that the good high-temperature strength and creep properties of these steels are due to the high lattice-friction stresses, which are a result of the very fine distribution of metal carbide (MC) precipitates and molybdenum in solid solution. In addition, a strong secondary wave of precipitation at approximately 650 °C was observed. This lattice friction stress maintained strength up to 600 °C.

Keywords creep, fire resistant, microstructure, steel, strength

1. Introduction

In recent years there has been a large increase in the number of multistory buildings constructed with steel frames due to a decrease in raw material prices and better productivity in the steel industry. Correspondingly, there has been an increase in research into fire engineering, with major findings being included in the publications of comprehensive Eurocodes EC3 and EC4 (Ref 1, 2). The main requirement of fire safety regulations is to ensure the safety of occupants and fire fighters, and in practice, to offer some protection to the building itself (Ref 1). It is well documented that conventional structural steels retain approximately 50 to 60% strength at around 550 °C (Ref 3-5). Fire protection is needed because the steels cannot withstand the temperatures experienced in real fires. Tests have been carried out on large-scale constructions at Cardington Laboratory in England as part of a European collaboration coordinated by the UK Building Research Establishment (BRE) and British Steel. Most of the steelwork involved was unprotected. Maximum steel temperatures between 690 and 1060 °C were recorded (Ref 6). If these temperatures are reached, then the limiting stress of the steel falls below the working stress and failure ensues. Thus, it is necessary to protect steelwork and ensure that such temperatures are not reached within the specified fire resistance period.

The main forms of fire protection are rigid boarding, spray, intumescent paint, concrete encasement, and flexible blanket; the first three dominate the market (Ref 4). Application of fire protection is a labor intensive activity. Most of the cost is derived from manual application rather than the material itself, and it can cost around 50% of the steel price (Ref 7). This means that reducing the amount, for example, thickness, of applied fire protection will not reduce the application cost significantly. The only ways to reduce the cost are either to eliminate the need for fire protection or to reduce the amount of steelwork that requires protection. Eliminating fire protection is advantageous in other ways, such as faster construction and the consequent cost saving, for example, from a quicker return on investment, as well as a reduction in site disruption and increased safety (Ref 7).

To eliminate fire protection, a fire resistant steel must retain a working stress higher than the applied stress at the given temperature, as well as having properties in other aspects adequate for structural purposes. The basic properties required of a fire-resistant structural steel are:

- High temperature strength retention
- Good ductility
- Good weldability
- Competitive cost

It has been estimated that retaining 60% of the room temperature strength at 800 °C would almost certainly guarantee an unprotected fire resistance of 30 min (Ref 8). This was confirmed by the recent computer modeling work of beam and floor slab structures by Sha (Ref 9). Thus, the ratio of the yield strength at a given temperature to the room-temperature yield strength, the yield strength ratio, is a useful parameter to compare steel performance at high temperatures.

Early research into fire-resistant microalloyed steels was carried out by the French steel company Creusot-Loire in the 1970s (Ref 10, 11). This was followed by further research in Australia (Ref 12) and Japan (Ref 13, 14) in the early 1990s. The latter steels were more effective, retaining 60% strength to temperatures of around 650 °C. Consequently, several fire-resistant steels are now manufactured commercially in Japan. Japanese construction standards are stricter than the Eurocodes, restricting the maximum steel temperature to that at which the steel retains two thirds of its room temperature yield strength, which for conventional steels is between 350 and 450 °C (Ref 13). Two fire-resistant steels manufactured by Nippon Steel are the subject of the present study; some of the work has been presented at conferences (Ref 15-17).

W. Sha, School of Civil Engineering, Queen's University of Belfast, Belfast BT7 1NN, UK; **F.S. Kelly,** Peter Brett Associates, Bridge Studios, 107A Hammersmith Bridge Road, London W6 9DA, UK; and **Z.X. Guo,** Department of Materials, Queen Mary and Westfield College, Mile End Road, London E1 4NS, UK. Contact e-mail: w.sha@qub.ac.uk.

2. Experimental Procedure

2.1 Composition

The compositions of the Nippon fire-resistant steels, which are referred to as the niobium and molybdenum steel, are given in Table 1.

2.2 Preparation of Microscopical Specimens

Optical Microscopy. Samples for optical microscopy were mounted in plastic resin and prepared according to Higgins (Ref 18), by grinding to 8 μm, followed by polishing to 1 μm. The samples were then etched using a 2% nital, as recommended by Vander Voort for low-carbon steels (Ref 19). Grain sizes were measured using the linear intercept method as described by Rostoker and Dvorak (Ref 20).

Transmission Electron Microscopy. Thin foil samples for transmission electron microscopy (TEM) were prepared by grinding the sample down to a thickness of 80 μm, after which 3 mm diameter samples were punched from the sheet, as recommended by Belk and Davies (Ref 21) . These 3 mm disks were then electropolished to transparency using a solution of 5% perchloric acid, 20% glycerol, and 75% methanol at –30 °C under 30 V.

Carbon extraction replicas for TEM were also prepared according to Belk and Davies (Ref 21). Heavily etched optical microscope specimens were carbon coated and then scratched in a square grid pattern. These were immersed in 10% nital until blistering of the carbon occurred after approximately 5 min. The samples were then removed from the acid, gently washed in ethanol, and immersed in a bath of distilled water. The carbon films were collected from the water surface onto copper grids and finished with careful drying.

Scanning Electron Microscopy. Fracture surfaces from tensile samples were examined using scanning electron microscopy (SEM). The fracture surface was cut from the sample approximately 3 mm from the fracture, carefully washed in ethanol, and attached to an aluminum disk. They were then carbon coated. Optically polished samples were also examined using SEM. Again, these were carbon coated or in some cases, gold coated, to improve the conduction over the sample surface.

2.3 Differential Scanning Calorimetry

Differential scanning calorimetry (DSC) tests were carried out on a Netzsch DSC 404 (Netzsch-Gerätebau GmbH & Co., Selb, Germany) using S-type thermocouples. Specimens were cut to 4 by 4 by 1 mm. After careful cleaning with alcohol, they were weighed, placed in Al_2O_3 crucibles, and inserted into the DSC furnace at ambient temperature. Tests were carried out without a reference sample at 2 °C/min. To limit the amount of oxidation, helium gas was used to provide a protective atmosphere. The furnace was purged with helium for 10 min before each test was started. An identical test was carried out with empty crucibles prior to sample tests to obtain a baseline. This was to correct for the instrumental contribution of each test and subsequently subtracted from each sample test to provide the sample signal.

2.4 Thermodynamic Calculations

Equilibrium calculations were carried out using the Thermo-Calc package, developed at the Royal Institute of

Table 1 Bulk compositions of the Nippon steels

	Element, wt%						
Steel	**C**	**Mn**	**Si**	**Mo**	**Nb**	**S**	**P**
Nb	0.11	1.14	0.24	0.52	0.03	0.02	0.009
Mo	0.1	0.64	0.1	0.51	…	0.05	0.009

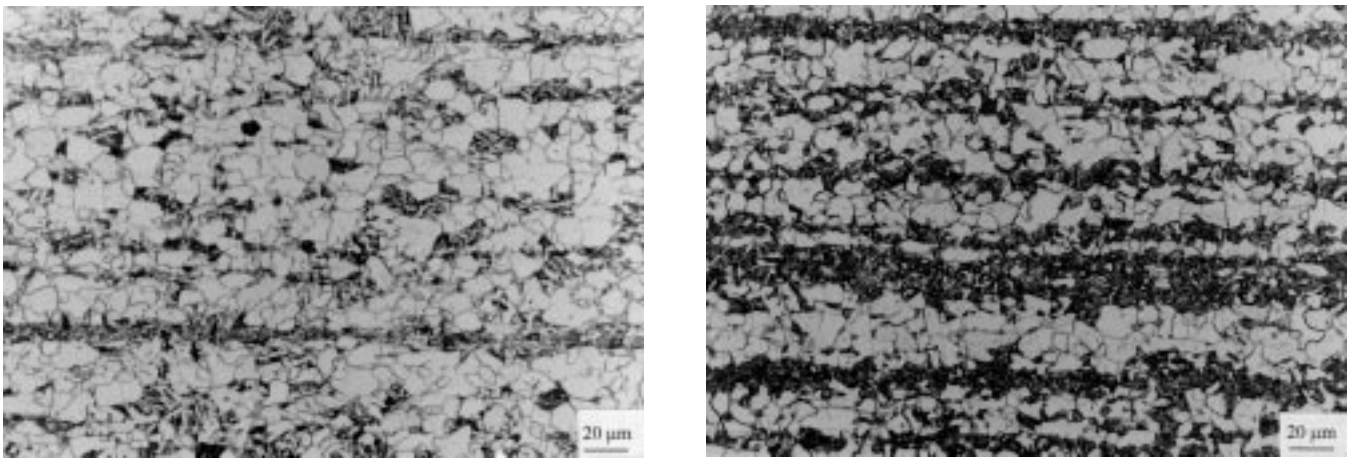

(a) **(b)**

Fig. 1 Optical micrographs of the niobium steel. (a) As received. (b) Heat treated for 30 min at 650 °C

Technology Stockholm. All phases in the Scientific Group Thermodata Europe (SGTE) Solution Database were entered, which included all common carbides and intermetallics. For some phases, however, the database may have insufficient consideration of solute partitioning.

3. Results and Discussion

3.1 Base Microstructure

Given the similarity of their compositions, it is not surprising that the two steels have similar base microstructures. Figures 1 and 2 show these microstructures in the as-received condition and after heat treatment at 650°C for 30 min for the niobium and molybdenum steel, respectively. The ferrite grain size in the as-received condition was around 6 μm for both steels and remained unchanged. There is an obvious effect of banding, which is more prevalent in the niobium steel than the molybdenum steel. Both steels have polygonal ferrite-pearlite structures containing approximately 80% ferrite. The remainder in both cases is made up of disrupted pearlite and a small amount of bainite. Figure 3 shows high magnification SEM images of this disrupted pearlite in the steels. It is not strictly lamellar, probably due to the partitioning of molybdenum to cementite. Thermo-Calc predictions have shown levels of molybdenum in the cementite of both steels (Table 2).

Table 2 Cementite compositions in the Nippon fire-resistant steels at 650 °C

	Element, at.%			
Steel	**C**	**Fe**	**Mn**	**Mo**
Nb	24.8	63.8	10.9	0.5
Mo	24.8	67.8	7.0	0.4

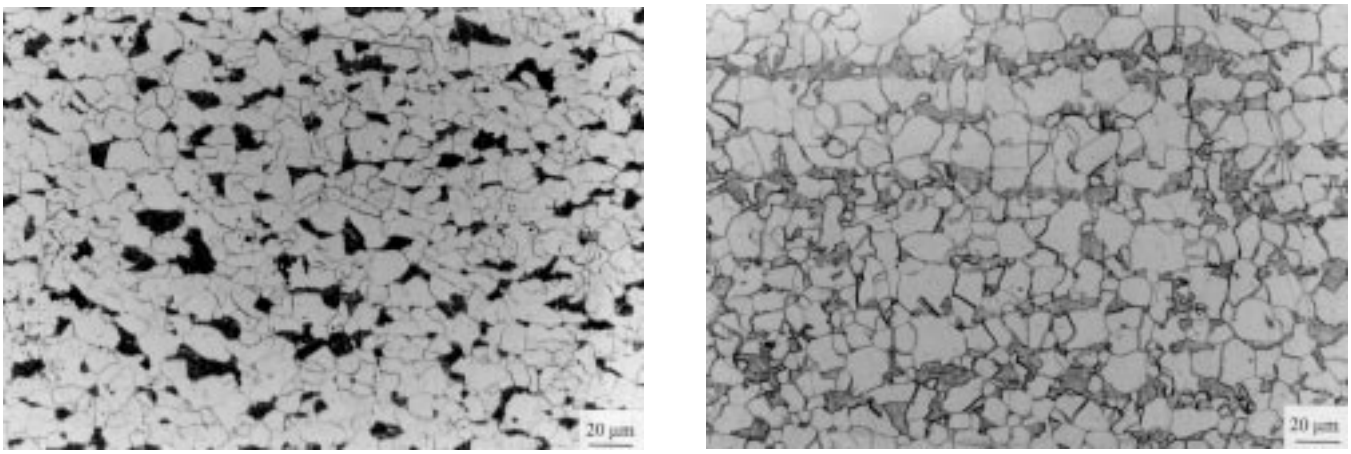

(a) **(b)**

Fig. 2 Optical micrographs of the molybdenum steel. (a) As received. (b) Heat treated for 30 min at 650 °C

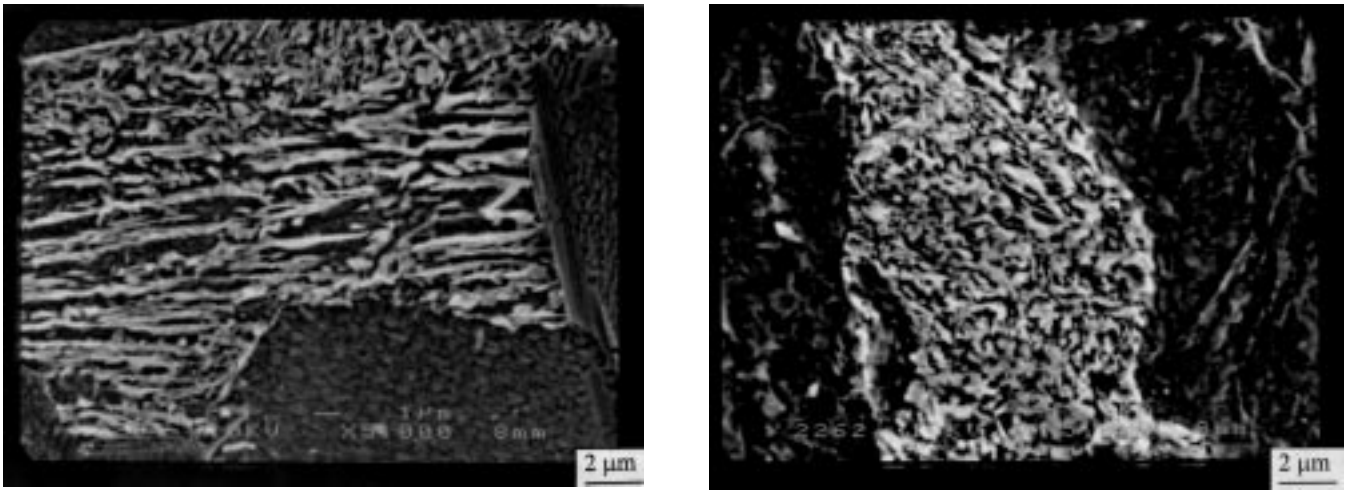

(a) **(b)**

Fig. 3 Scanning electron micrographs of the typical pearlite morphology in the as-received condition. (a) Niobium steel. (b) Molybdenum steel

Honeycombe and Bhadeshia stated that molybdenum addition substantially lowers the rates of nucleation and growth of pearlite in steels, as well as altering the morphology (Ref 22). Thus, the levels of molybdenum in the cementite of both steels may account for the disrupted morphology. Thermo-Calc calculations also showed that the manganese level of cementite in both steels decreased with increasing temperature.

The eutectic temperatures were obtained from DSC analysis as 733 °C for both steels. The values predicted by Thermo-Calc were 693 °C for the niobium steel and 708 °C for the molybdenum steel.

3.2 Precipitation

It has been shown by Wang et al. (Ref 23) that differentiating between Mo_2C and MoC is extremely difficult using TEM electron diffraction. Therefore, although both Mo_2C and MC were identified in either Nippon steel by diffraction, these results are subject to a degree of uncertainty. Wang et al. also reported that MC and Mo_2C coexisted in the same steel. Equilibrium precipitation predicted by Thermo-Calc is NbC ($Nb_{40}Mo_7C_{53}$) and MoC in the niobium steel and MoC in the molybdenum steel. The calculations showed that these are the stable carbides below approximately 650 °C. It is unclear why the NbC-type precipitate deviates from stoichiometry. Cottrell (Ref 24) stated that MC_x has insignificant deviation from the stoichiometric composition, which only occurred when $x < 1$. However, Kneissl et al. (Ref 25) reported MC precipitates in which carbon was above the stoichiometric composition in an atom-probe, field-ion microscopy (APFIM) study of steel alloyed with low levels of chromium, molybdenum, and niobium. It can be noted that Thermo-Calc predicts no iron in the MC precipitates of these steels. Of note is the effect of the mixed composition of precipitates. Due to their thermal stability, fine size, dense distribution, and slow rate of coarsening, MC-type carbides of mixed composition were reportedly the more stable species of carbides in high-speed steels. They were thus thought to be the optimum carbide type for high temperature strength, according to Wang et al. (Ref 23).

Precipitates in both steels were observed at grain boundaries, on dislocations, and in the matrix. Precipitates in the niobium steel tend to be spherical with some larger cuboidal particles. In the molybdenum steel, both large and small particles are cuboidal. Figure 4 shows transmission electron micrographs of typical carbon extraction replicas displaying the precipitate morphology.

Precipitate size distributions before and after heat treatment were assessed from carbon-extraction replica images (Fig. 5). In the as-received condition, the niobium steel exhibits a small peak at 40 to 50 nm, suggesting that there are two distributions of precipitate. These larger particles may be NbC precipitates, which precipitated during rolling; whereas the smaller particles could be the distribution of MoC precipitates. The MoC has a higher solubility than NbC, and thus precipitates at a lower temperature, leading to finer dispersion (Ref 22). There is a decrease in the average precipitate size after annealing for 30 min at 650 °C from 41 to 34 nm in the niobium steel and from 34 to 28 nm in the molybdenum steel. The most frequently occurring precipitate sizes were 4.1 nm for both steels in the as-received condition and 1.6 and 2.5 nm for the niobium and molybdenum steel, respectively, after the heat treatment. These results imply that there may be a secondary hardening reaction due to precipitation in both steels. Such a phenomenon was also reported by Wang et al. (Ref 23) for MC precipitates in high-speed steels.

Transmission electron microscopy study of thin foils and hardness testing of the steels have shown that further precipitation does occur at 650 °C. The precipitate number density, estimated assuming a foil thickness of 100 nm, increased from 1.1×10^{14} to $1.3 \times 10^{14}/cm^3$ and from 8.5×10^{13} to $1.3 \times 10^{14}/cm^3$ for the niobium and molybdenum steels, respectively, after the heat treatment. This also corresponded with a peak in hardness after heat treatment at this temperature (Ref 26). However, the increase of hardness is not affected by the aging time, up to 3 h.

3.3 Lattice Friction Stress

Values of lattice friction stress for these steels can be calculated from the Hall-Petch equation:

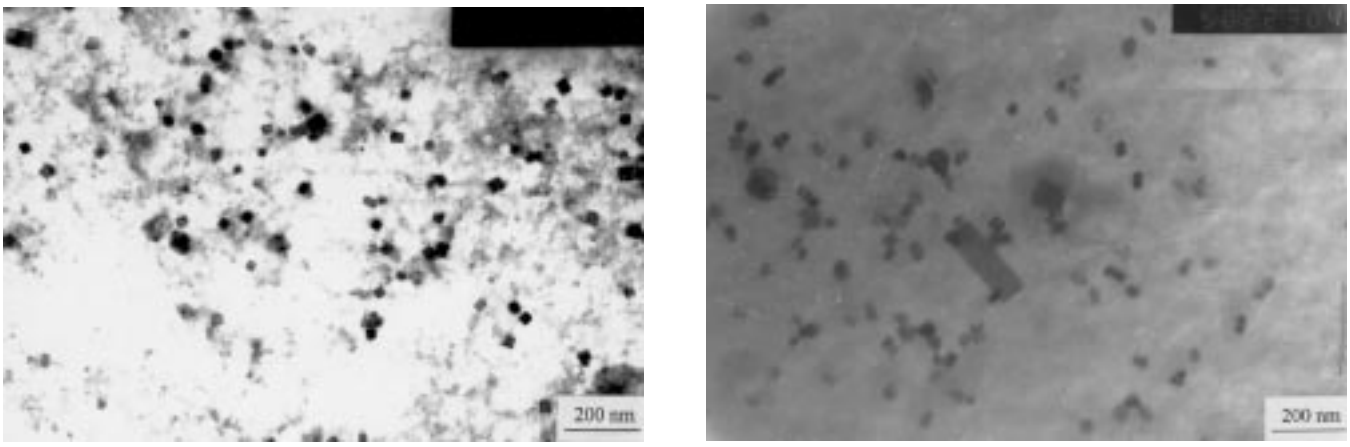

(a) **(b)**

Fig. 4 Transmission electron micrographs of carbon extraction replicas showing the precipitate morphology. (a) Niobium steel. (b) Molybdenum steel

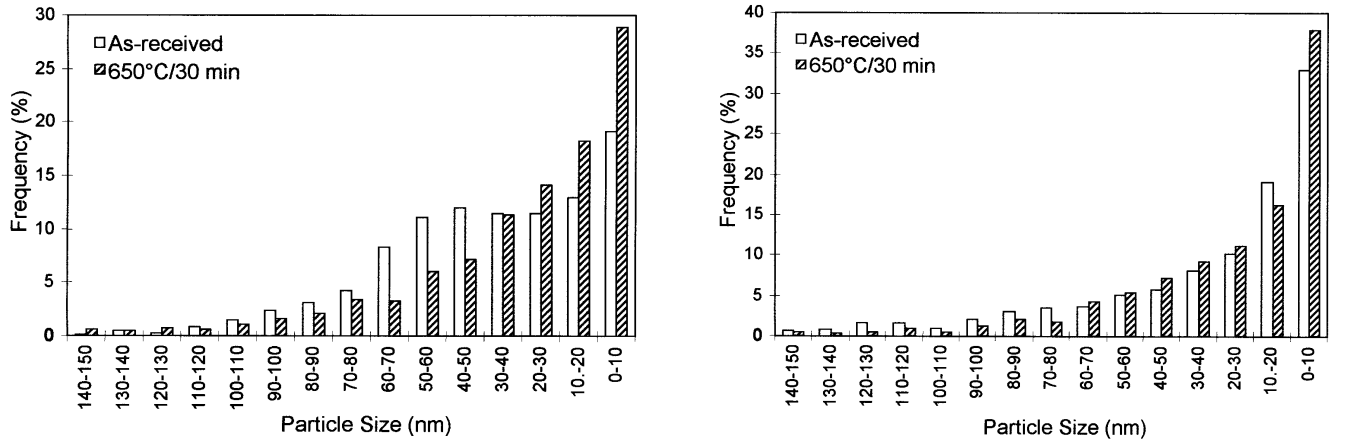

Fig. 5 Size distribution of the precipitates in the as-received condition and after heat treatment at 650 °C for 30 min. (a) Niobium steel. (b) Molybdenum steel

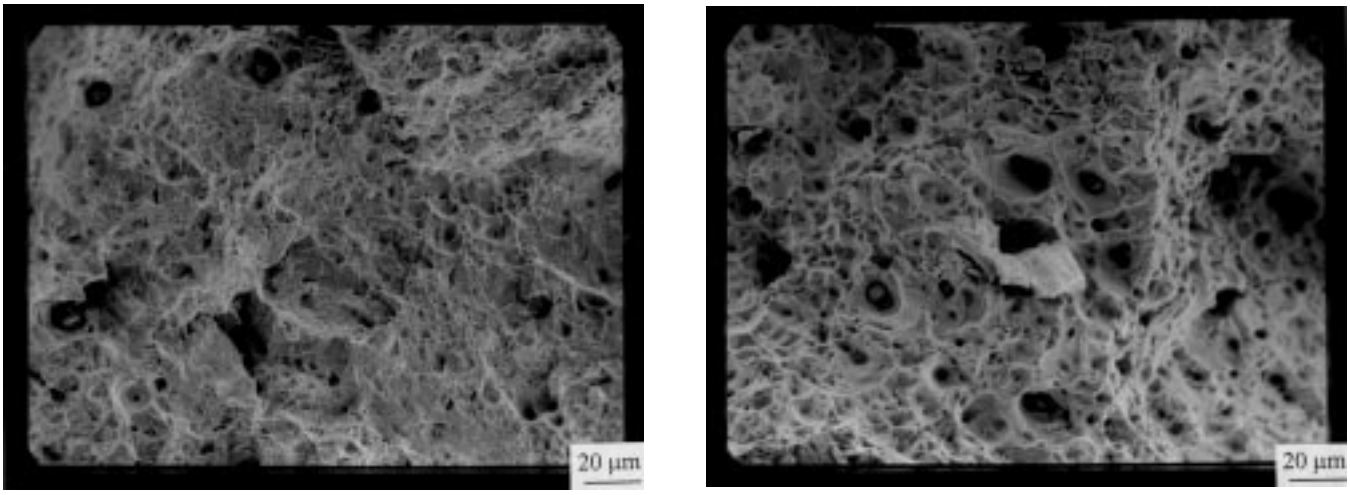

Fig. 6 Fractographs of the niobium steel. (a) Tested at room temperature. (b) Tested at 600 °C

$$\sigma_y = \sigma_i + k_y d^{-1/2}$$

where σ_y is the yield stress and σ_i is the friction stress, representing the stress required to move free dislocations along slip planes in body-centered cubic (bcc) crystals. The parameter k_y reflects the difficulty of transmitting slip across grain boundaries and is around 17.4 N/mm$^{3/2}$ according to Pickering and Gladman (Ref 27). The d is the average ferrite grain size in millimeters. The friction stress values were calculated to be 170 MPa for the niobium steel, 157 MPa for the molybdenum steel, based on yield strengths measured in tensile tests (Ref 26) and grain sizes measured in the present work. The high lattice friction stresses are due to the distribution of very fine carbide precipitates and the considerable amount of molybdenum in solid solution. Thus, bypassing these obstacles must occur for dislocations to move through the matrix. In the case of edge dislocations, the process of climb is slow because the rate-controlling process during dislocation climb is atomic diffusion.

There are several strengthening mechanisms contributing to the lattice friction stress (Ref 28):

$$\sigma_i = \sigma_0 + \sigma_{ss} + \sigma_{ppt} + \sigma_d$$

where σ_0 is the intrinsic strength of the ferrite lattice (63.7 MPa) (Ref 28); σ_{ss} is the contribution from solid solution strengthening by substitutional elements, 32 (wt% Mn) + 83 (wt% Si) + 11 (wt% Mo) (Ref 29) ; and σ_d is the strengthening from dislocations. The σ_d is negligibly small because the finish rolling temperature was above the Ar_3 transformation temperature. The parameter σ_{ppt} is the contribution from precipitation calculated from the Ashby-Orowan model (Ref 25):

$$\sigma_{ppt} = \frac{1}{1.18}\left(\frac{1.2Gb}{\pi L}\right)\ln\frac{x}{2b}$$

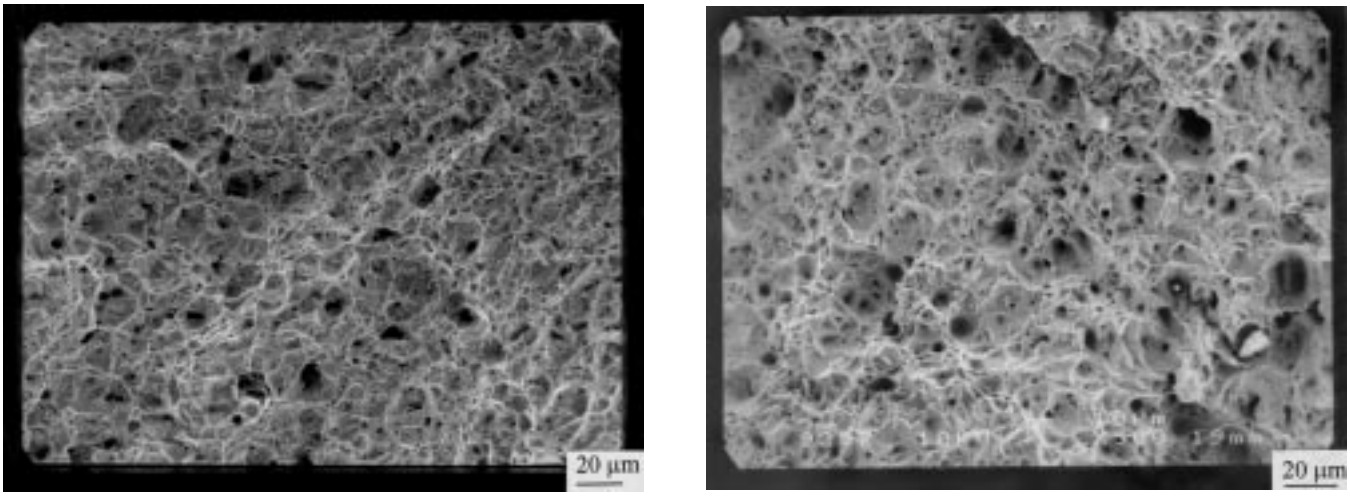

(a) **(b)**

Fig. 7 Fractographs of the molybdenum steel. (a) Tested at room temperature. (b) Tested at 600 °C

where G is the shear modulus (80.3 GPa) (Ref 30); b is the Burger's vector in the slip direction (0.25 nm); $x = d(2/3)^{1/2}$, d is the mean particle diameter; and L is the interparticle spacing ($n^{-1/3} - x$, where n is the precipitate number density). The lattice friction stresses calculated from these equations using precipitation size and number density data were both within 5% of those obtained directly from the Hall-Petch equation, as in the beginning of this section, showing the accuracy of the various experimental data obtained in this program.

An applied stress of 220 MPa, approximately 60% of the room temperature of the steel yield stress, is a typical load in practical applications. For this stress, the parameter σ/G is 3.5×10^{-3}, where G is the shear modulus (63 GPa at 600 °C) (Ref 31). Dieter stated that the mechanism of secondary creep depends on the applied stress (Ref 32). For values of $10^{-4} < \sigma/G < 10^{-2}$, the main mechanism is dislocation creep, where gliding dislocations overcome obstacles by climb, assisted by diffusion of vacancies or interstitial elements. Thus, this is thought to be the main mechanism of creep for these steels. The high friction stress of the steels strongly resists dislocation movement, and, hence, the steels retain a high strength at elevated temperatures.

3.4 Fracture Surfaces

Fracture surfaces for both steels were formed by coalescence of microvoids initiated at inclusions, characteristic of ductile fracture. Typical scanning electron micrographs of fracture surfaces are shown in Fig. 6 and 7 for the niobium steel and the molybdenum steel, respectively, at room temperature and at 600 °C. Inclusions in both steels are typically calcium aluminates or mixed inclusions containing sulfur, calcium, aluminum, manganese, and silicon. The latter is likely to be clusters of MnS and calcium and aluminum silicates.

4. Conclusions

The good high-temperature strength and creep properties of Nippon steels are due to the high lattice friction stresses, which are a result of the very fine distribution of MC precipitates, molybdenum in solid solution, and a strong secondary wave of precipitation at approximately 650 °C. This lattice friction stress maintains strength up to 600 °C when grain boundary sliding begins.

References

1. Structural Fire Design, "BS ENV 1993: Eurocode 3: Design of Steel Structures" (including UK NAD), Part 1.2, British Standards Institution, London, 1996
2. Structural Fire Design, "BS ENV 1994: Eurocode 4: Design of Composite Steel and Concrete Structures" (including UK NAD), Part 1.2, British Standards Institution, London, 1996
3. R.M. Lawson and G.M. Newman, *Structural Fire Design to EC3 & EC4, and Comparison with BS 5950*, The Steel Construction Institute, Ascot, 1996
4. *Fire Resistance of Steel-Framed Buildings*, British Steel Sections Plates and Commercial Steels, Steel House, Redcar, UK, 1997
5. T.J. MacGinley and T.C. Ang, *Structural Steelwork: Design to Limit State Theory*, 2nd ed., Butterworth Heinemann, Oxford, 1992, p 10
6. D.B. Moore and T. Lennon, Fire Engineering Design of Steel Structures, *Progress in Structural Engineering and Materials*, Vol 1 (No. 1), 1997, p 4-9
7. *Steel or Concrete: The Economics of Commercial Buildings*, British Steel Sections Plates and Commercial Steels, Steel House, Redcar, UK, 1996, 15 pages
8. J.T. Robinson, British Steel Sections Plates and Commercial Steels, Steel House, Redcar, UK, Private communication, 1996
9. W. Sha, Fire Resistance of Floors Constructed with Fire-Resistant Steels, *J. Struct. Eng.*, Vol 124 (No. 6), 1998, p 664-670
10. "Recherce et Mise au Point d'Acier Moyennment Allies a Resistance au Feu Renforcee: Etude Theorique des Caracteristiques Optimals," 75-61542-06-223-75-01, Raport Techniques No. 1, Creusot-Loire, Usine du Creusot, Sept 1976 (in French)
11. "Recherche et Mise au Point d'Acier Moyennment Allies a Resistance au Feu Renforcee, Determination des Caracteristiques a Chaud des Aciers," 75-61542-06-223-75-01, Raport Techniques No. 2, Creusot-Loire, Usine du Creusot, Aug 1977 (in French)

12. M. Assefpour-Dezfuly, B.A. Hugaas, and A. Brownrigg, Fire Resistant High-Strength Low-Alloy Steels, *Mater. Sci. Technol.*, Vol 6 (No. 12), 1990, p 1210-1214
13. R. Chijiiwa, H. Tamehiro, A. Yoshie, K. Funato, Y. Yoshida, Y. Horii, and R. Uemori, Development and Practical Application of Fire-Resistant Steel for Buildings, *HSLA Steels '95 Conf. Proc.*, G. Liu, H. Stuart, H. Zhang, and C. Li, Ed., China Science and Technology Press, Beijing, 1995, p 584-589
14. "Kawasaki Steel Technical Report," No. 29, Nov. 1993, Kawasaki Steel
15. W. Sha and F.S. Kelly, Mechanical Property and Microstructure of Structural and Fire Resistant Steels, *Proceedings of the Third Pacific Rim International Conference on Advanced Materials and Processing*, Vol 1, M.A. Imam, R. DeNale, S. Hanada, Z. Zhong, and D.N. Lee, Ed., The Minerals, Metals, and Materials Society, 1998, p 199-204
16. W. Sha, P.J. Blair, and F.S. Kelly, Tensile Properties of Mo and Mo-Nb Microalloyed Fire Resistant Steels, *Proceedings of the Third Pacific Rim International Conference on Advanced Materials and Processing*, Vol 1, M.A. Imam, R. DeNale, S. Hanada, Z. Zhong, and D.N. Lee, Ed., The Minerals, Metals, and Materials Society, 1998, p 247-252
17. F.S. Kelly and W. Sha, Mechanical Properties of Fire-Resistant Steels for Construction, *Euromat 97—Proceedings Fifth European Conference on Advanced Materials and Processes and Applications: Materials, Functionality and Design*, Vol 1, L.A.J.L. Sarton and H.B. Zeedijk, Ed., Netherlands Society for Materials Science, Zwijndrecht, 1997, p 35-40
18. R.A. Higgins, *Engineering Metallurgy*, 6th ed., Edward Arnold, London, 1993
19. G.F. Vander Voort, *Metallography: Principles and Practice*, McGraw-Hill, 1994, p 632
20. W. Rostoker and J.R. Dvorak, *Interpretation of Metallographic Structures*, 2nd ed., Academic Press, 1977, p 222
21. J.A. Belk and A.L. Davies, *Electron Microscopy and Microanalysis of Metals*, Elsevier, 1968, p 28-62
22. R.W.K. Honeycombe and H.K.D.H. Bhadeshia, *Steels: Microstructure and Properties*, 2nd ed., Edward Arnold, London, 1995
23. R. Wang, H. Andren, H. Wisell, and G. Dunlop, The Role of Alloy Composition in the Precipitation Behavior of High-Speed Steels, *Acta Metall. Mater.*, Vol 40 (No. 7), 1992, p 1727-1738
24. A. Cottrell, *Chemical Bonding in Transition Metal Carbides*, The Institute of Materials, London, 1995, p 77
25. A.C. Kneissl, C.I. Garcia, and A.J. DeArdo, Characterization of Precipitates in HSLA Steels, *Proceedings of Second International Conference on HSLA Steels: Processing, Properties and Applications*, G. Tither and S.H. Zhang, Ed., The Minerals, Metals, and Materials Society, 1990, p 99-105
26. F.S. Kelly and W. Sha, A Comparison of the Mechanical Properties of Fire-Resistant and S275 Structural Steels, *J. Constr. Steel Res.*, Vol 50 (No. 3), 1999, p 223-233
27. F.B. Pickering and T. Gladman, *Iron and Steel Institute Special Report*, Vol 81, 1963, p 10
28. S.-C. Wang, The Effect of Titanium and Reheating Temperature on the Microstructure and Strength of Plain-Carbon, Vanadium-Microalloyed, and Niobium-Microalloyed Steels, *J. Mater. Sci.*, Vol 25 (No. 1A), 1990, p 187-193
29. D.T. Llewellyn, *Steels: Metallurgy and Applications*, 2nd ed., Butterworth-Heinemann, Oxford, 1994, p 68
30. A. Cottrell, *An Introduction to Metallurgy*, 2nd ed., The Institute of Materials, London, 1995
31. *Metals Handbook*, 9th ed., American Society for Metals, 1978
32. G. Dieter, *Mechanical Metallurgy*, 3rd ed., McGraw-Hill, Singapore, 1987